Odyssey Papers 33

The Wreck of the First Rate Warship the *Victory*, Western English Channel: Site 25C Sediment Analysis

Anthony R. Prave, Donald A. Herd, Angus C. Calder & Stuart G. Allison
Centre for Earth Resources St. Andrews, University of St. Andrews, Scotland

Four sedimentological and geological samples (GO1, GO2, GO3, GO4) were recovered in February 2012 from the outer perimeter of the wreck of the *Victory* (1744) in the Western English Channel using the Remotely-Operated Vehicle Zeus. These were subjected to grain size and bulk geochemical compositional analyses at the Centre for Earth Resources St. Andrews (CERSA), Scotland, using a Beckman-Coulter LS-230 particle size analyser, a X-Ray Fluorescence Spectrometry (XRF) and a X-Ray Diffraction (XRD), as well as imaging using a Keyence VHX 2000 3D digital microscope.

Samples GO1, GO2 and GO3 contained abundant material between *c.* 1-2mm and larger. Finer than coarse sand comprised only around 1-2% by volume of the samples, while 38-59% by volume proved to be very coarse sand and gravel particles. As such, site 25C is not an optimum environmental setting for the anaerobic preservation of cultural remains. The entire sedimentological samples give the impression of being extensively sorted and dynamic, a profile which is also evident from side-scan sonar and multibeam imagery of large bedforms indicative of a mobile substrate.

1. Introduction

The Centre for Earth Resource St. Andrews (CERSA) received four samples, GO1, GO2, GO3 and GO4, for grain size and bulk geochemical compositional analyses associated with the wreck of the First Rate English warship, the *Victory* (site 25C), lost in the Western English Channel in October 1744. The submitted data included relevant site maps and digital photography. The samples were obtained from two peripheral site locations, GO1 to the south and the others to the northwest, and were described visually as:

- GO1 (Context 1): mixed fine to large-grained sand and fine to large shell fragments.
- GO2 (Context 2): mixed fine to large-grained sand, but displays a dark gray color due to sub-surface burial in a deoxygenated environment.
- GO3 (Context 3): small stones, pebbles and flint nodules emerging in association with Context 1 deposits.
- GO4 (Context 4): hardpan composed of stone and flint nodules representing the lowest stratum on which archaeological remains are deposited on the site.

Samples GO1, GO2 and GO3 were subject to three types of analyses. The first was to determine accurately and precisely the grain size distribution using a Beckman-Coulter LS-230 particle size analyser, which passes a laser beam of known wavelength through a suspension of particles. The light becomes scattered (diffracted) and its pattern and intensity is then measured and fitted to a theoretical model to calculate the size of particles. The LS-230 measures volume percent in fractions ranging from 0.4 to 2000 microns. The second analysis involved XRF/D analyses to define elemental compositions and mineralogy. X-Ray Fluorescence Spectrometry (XRF) is a non-destructive analytical technique used to identify elements (typically Na through U) in solid, powdered and liquid samples and to determine their concentrations at trace levels to parts per million. Thirdly, X-Ray Diffraction (XRD) is a versatile technique that informs on the composition and crystallographic structure of natural (minerals) and man-made material. Samples are powdered and exposed to X-rays, whose diffraction pattern identifies the unique arrangement of atoms in a crystal structure.

Sample GO4 consisted of gravels and cobbles and those, along with the 1mm and larger material from the other three samples, were examined visually. Donald Herd undertook the grain size analyses, Angus Calder performed the XRF/D work, Stuart Allison identified the shelly material and Anthony Prave compiled and interpreted the data and wrote this report.

Sediment Type	GO1 (%)	GO2 (%)	GO3 (%)
Clay	0.17	0.50	0.19
Silt	0.07	0.29	0.09
Very Fine Sand	0.11	0.47	0.15
Fine Sand	0.08	0.39	0.12
Medium Sand	0.13	0.59	0.21
Coarse Sand	46.57	60.22	40.23
Very Coarse Sand	22.15	23.19	27.90
Gravel	30.71	14.34	31.14

Table 1. Grain size distribution by volume percent for samples GO1, GO2 and GO3.

2. Grain Size Analyses: 1mm & Less

A. Samples GO1, GO2, GO3

Samples G01, G02 and G03 were first sieved to separate the particles into size fractions of greater than and less than 1mm. The latter were then analyzed for grain size distributions using the Beckman-Coulter LS-230 laser granulometer. Complete grain size results are presented in Appendix A, summarized in Table 1 and illustrated graphically in Figs. 1-2.

The size fractions were grouped using the Wentworth particle size diameter classification: clay (< 0.0039mm), silt (0.0039mm to 0.0625mm), very fine sand (0.0625mm to 0.125mm), fine sand (0.125mm to 0.25mm), medium sand (0.25mm to 0.5mm), coarse sand (0.5mm to 1mm), very coarse sand (1mm to 2mm) and gravel (> 2mm). As shown in Table 1 and Fig. 1, the combined size fractions finer than coarse sand comprise only *c*. 1-2% by volume in each of the three samples. Hence, these size fractions were added together to form the pie charts (Fig. 2). The results show that sample GO3 is the overall coarsest, being composed of *c*. 59% by volume of very coarse sand and gravel particles, followed by sample GO1 with *c*. 53% by volume of very coarse sand and gravel. Sample GO2 is the relative finest, with the very coarse sand and gravel fractions comprising *c*. 38% by volume of the particles (Table 1).

The particle-size distributions do not appear to be overly remarkable, although there is an interesting inter-sample grain size trend given their locations on the seabed in the vicinity of the wreck (Fig. 3). The 2012 multibeam image shows that the western seabed is marked by relatively small-scale (dcm-scale sizes) and somewhat disorganised bedforms that pass rather sharply into larger, meter-scale bedforms. In the vicinity of the wreck, the larger bedforms are 3D large ripples (i.e. sinuous-crested 'dunes' exhibiting meter-scale spacings). Beyond the wreck, these transition into more straight-crested, large 2D bedforms (straight-crested sand 'waves' with meter-scale spacings). The asymmetry of the bedforms indicates that the current is dominantly unidirectional, such that sediment transport is directed obliquely from southwest towards northeast (in the direction of the shallowing).

The genesis of bed configurations (the overall association of bedforms on a given substrate) is largely a function of the first-order variables of flow depth, flow velocity and grain size. Given that the color-coding on the multibeam sonar image indicates decreasing water depth from west to east (Fig. 3), then it is likely that there was a concomitant increase in current strength (greater velocity) to account for the transition from smaller-scale bedforms to larger sand waves/dunes in the coarse sand and gravel materials. The genesis of the 3D large bedforms in the vicinity of the wreck perhaps reflects constriction of currents around the wreckage causing a local enhancement of flow velocities upward into the bed-stability field for 3D large ripples.

One additional aspect of the grain size analyses that is noteworthy is the relative proportion of fine sand between samples GO1-GO3 (Fig. 4). As noted previously, samples GO1 and GO3, relative to sample GO2, have lesser proportions of fine sands (albeit the overall amount of finer grained material remains relatively minor). Samples GO1 and GO3 are within or proximal to the zone of transition from the small- to large-scale bedforms; their overall coarser grain size distribution may in part reflect a winnowing effect and removal of the finer-sized material due to the (hypothesised) shift to greater flow velocities as indicated by the change from smaller to larger bedforms. Sample GO2, which derives from outside this zone, retains the minor finer sizes (Figs. 1-2).

3. Grain Size Analyses: Greater than 1mm

Samples GO1, GO2 and GO3 have abundant material between *c.* 1-2mm and larger. This magnitude is beyond the range limit for laser granulometric analysis using the

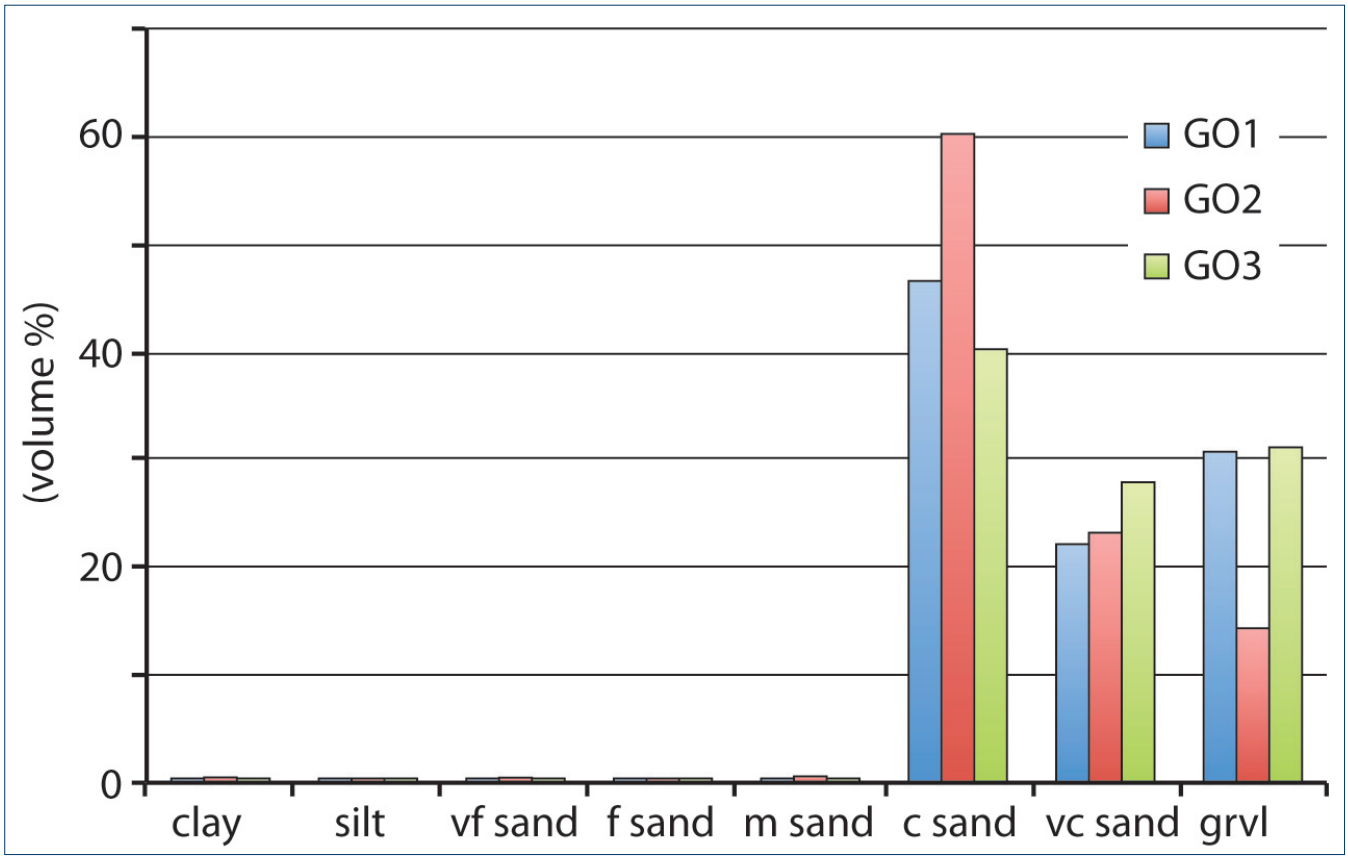

Fig. 1. Grain size distributions of samples GO1, GO2, GO3 as histograms.

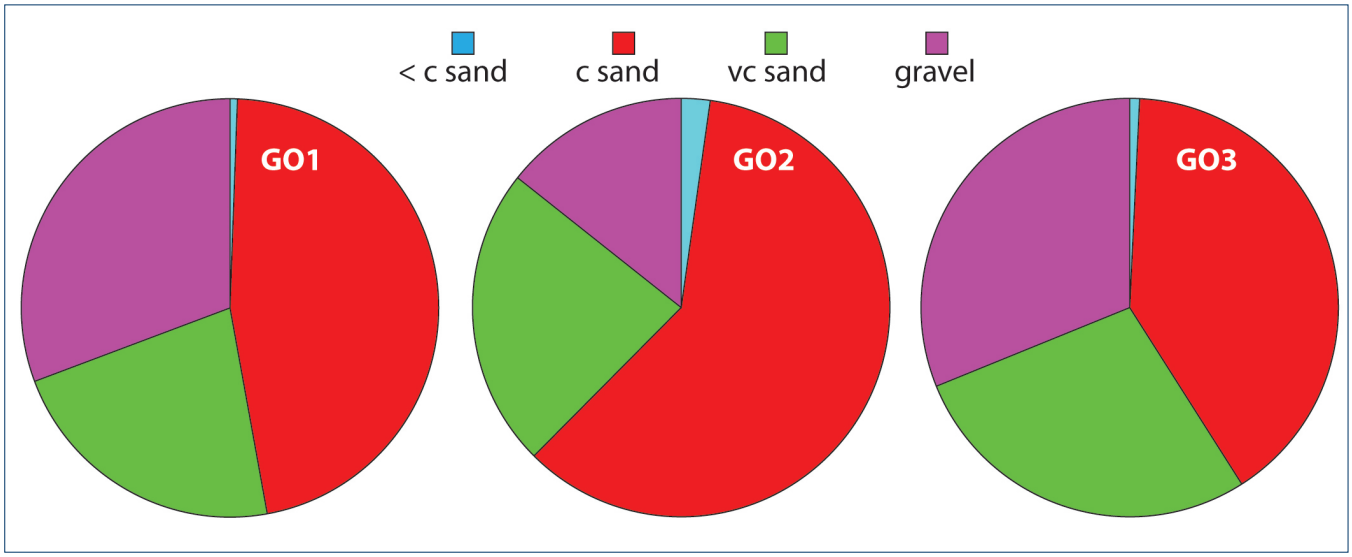

Fig. 2. Pie-chart grain-size distributions for samples GO1, GO2, GO3 showing the overall coarse nature of the sediment. Note the relatively finer overall size of GO2 compared to GO1 and GO3.

Siroquant Semi-Quant (wt%)	GO1 (%)	GO2 (%)	GO3 (%)
Quartz	19	13	19
Aragonite	13	12	15
Calcite	39	40	36
Mg-Calcite	28	34	29
Halite	1	1	1
Plagioclase	1	--	--

Table 2. Semi-quantitative XRD results for samples GO1, GO2 and GO3.

	Na_2O	MgO	Al_2O_3	SiO_2	P_2O_5	SO_3	K_2O	CaO	TiO_2	MnO	Fe_2O_3
	%	%	%	%	%	%	%	%	%	%	%
GO1	0.82	1.03	0.64	20.42	<0.02	<0.01	0.22	40.85	0.03	0.02	0.49
GO2	0.94	1.19	0.69	13.12	<0.02	0.04	0.21	44.41	0.04	0.01	0.42
GO3	0.89	0.92	0.72	19.29	<0.02	0.12	0.17	41.84	0.03	0.01	0.64

Table 3. XRF results for major oxides on samples GO1, GO2 and GO3.

	V	Cr	Co	Ni	Cu	Zn	Ga	Ge	As	Se	Br
	ppm	ppm	ppm	ppm	ppm	ppm	ppm	ppm	ppm	ppm	ppm
GO1	7	7	< 5	1	47	6	< 1	< 2	< 3	< 2	4
GO2	3	12	< 5	1	33	8	< 1	< 2	< 3	< 2	6
GO3	4	7	< 5	2	57	5	1	< 2	< 3	< 2	4
	Rb	**Sr**	**Y**	**Zr**	**Nb**	**Mo**	**Ag**	**Cd**	**In**	**Sn**	**Sb**
	ppm	ppm	ppm	ppm	ppm	ppm	ppm	ppm	ppm	ppm	ppm
GO1	5	1980	5	13	2	< 2	< 2	< 2	< 2	< 2	< 2
GO2	1	2103	4	10	2	< 2	< 2	< 2	< 2	< 2	< 2
GO3	3	1948	5	24	2	< 2	< 2	< 2	< 2	< 2	< 2
	I	**Cs**	**Ba**	**La**	**Ce**	**Pr**	**Nd**	**Pb**	**Th**	**U**	
	ppm	ppm	ppm	Ppm	ppm	ppm	ppm	ppm	ppm	ppm	
GO1	18	2	42	< 5	< 5	< 5	< 5	11	2	< 1	
GO2	13	2	31	< 5	< 5	< 5	< 5	28	2	< 1	
GO3	12	4	33	< 5	< 5	< 5	< 5	13	1	< 1	

Table 4. XRF results for trace elements on samples GO1, GO2 and GO3.

Beckman-Coulter LS230. Consequently, this material was examined visually. With the exception of the lithic fragments described below, much of the material consists of broken and abraded bioclastic fragments dominated by epifauna forms such as bivalves and bryozoans (Fig. 5).

A. Bioclastic Components

Sample GO1, GO2, GO3

Sample GO1 consists of *c*. 70-75% highly abraded bivalve mollusc fragments, mostly indet but includes pectinids. There is around 10-15% of lightly abraded smaller bivalve disassociated valves and these are mainly thin-shelled, shallow-infaunal, shallow-burrowing forms such as *Cerastoderma sp*. and Tellinids. A further *c*. 10-15% of the material consists of abraded and separated barnacle plates (*sp. indet.*). Minor to rare amounts of regular echinoid plates and spines, encrusting or erect bryozoan (including *Cellaria sp*.) and gastropods are also present.

Sample GO2 is comprised of around 50% fragments of bryozoan colonies, including disaggregated and variously abraded, jointed, erect cylindrical calcareous colonies of the bryozoan *Cellaria sp*. and more fragmentary encrusting bryozoan forms (*species indet.*). Abraded and fragmental

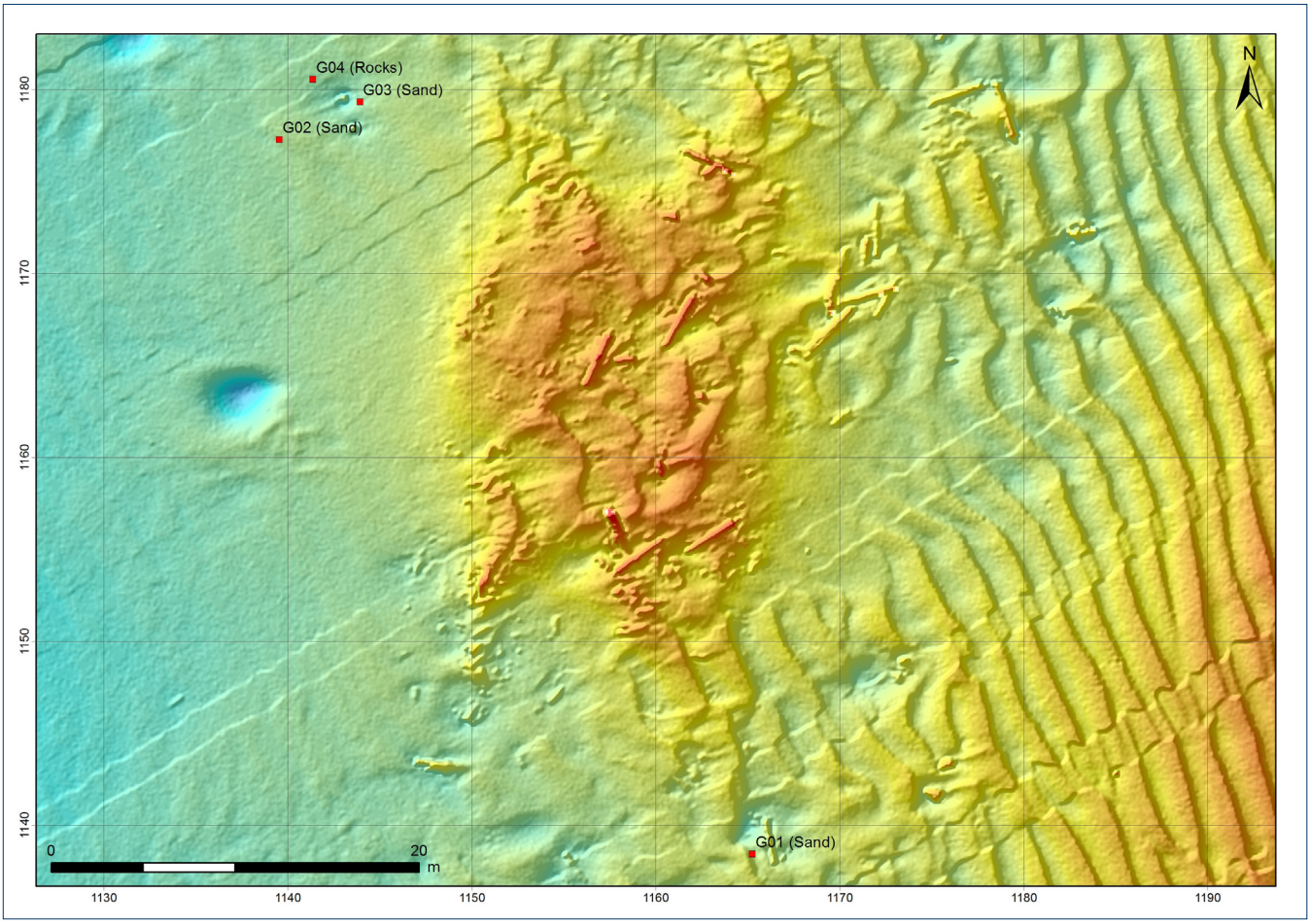

Fig. 3. Multibeam sonar image of the seabed at site 25C showing the position of the wreck in relation to the peripheral locations of samples GO1-4.

bivalve mollusc fragments, including ribbed epifaunal pectinid (scallop) forms, make up *c.* 40% of the remainder of the sample. There are a few abraded crustacean fragments, lightly abraded smaller bivalve disassociated valves (forms similar to those in sample GO1, namely *Cerastoderma sp*. and Tellinids), and some small, well-preserved infaunal irregular echinoid tests of *Echinocyamus sp*. Rare, abraded and separated barnacle plates (*sp indet.*) and one regular echinoid (*Echinus*.) fragment was observed.

Sample GO3 consists of around 40-45% abraded and fragmental bivalve mollusc fragments, including ribbed epifaunal pectinid (scallop) forms, *c.* 35-40% fragments of bryozoan colonies (similar to samples GO1 and GO2), which are largely disaggregated and variously abraded, jointed, erect cylindrical colonies of *Cellaria sp*. and more fragmentary encrusting forms (*species indet.*), and *c.* 10-15% of lightly to non-abraded disassociated valves of smaller bivalves (mainly the thin-shelled, shallow-infaunal, shallow-burrowing forms of *Cerastoderma sp*. and Tellinids). Overall, sample GO3 has experienced more abrasion than the other two samples.

In summary, the fauna suggest normal marine salinities, water depths associated with normal wave base and away from centers of high rates of deposition to explain the high concentrations of carbonate material and fairly high rates of reworking and abrasion of the epifauna. It is dominated by transported shallow water epifauna consisting of bivalves, bryozoan, barnacles, crustaceans and regular echinoids. The few, small, well preserved, thin-shelled infaunal elements (Tellinids and echinoids) may reflect the thinness of sediment and its susceptibility to temporary removal from the sites. The bryozoan *Cellaria sp*. can withstand wave action along with slow silt deposition and its preservation suggests it is local to the area, along with the infauna. The striking lack of gastropods is noteworthy (and puzzling). Lastly, the relative lack of borings on the shell surfaces suggests high rates of reworking and abrasion (strong currents).

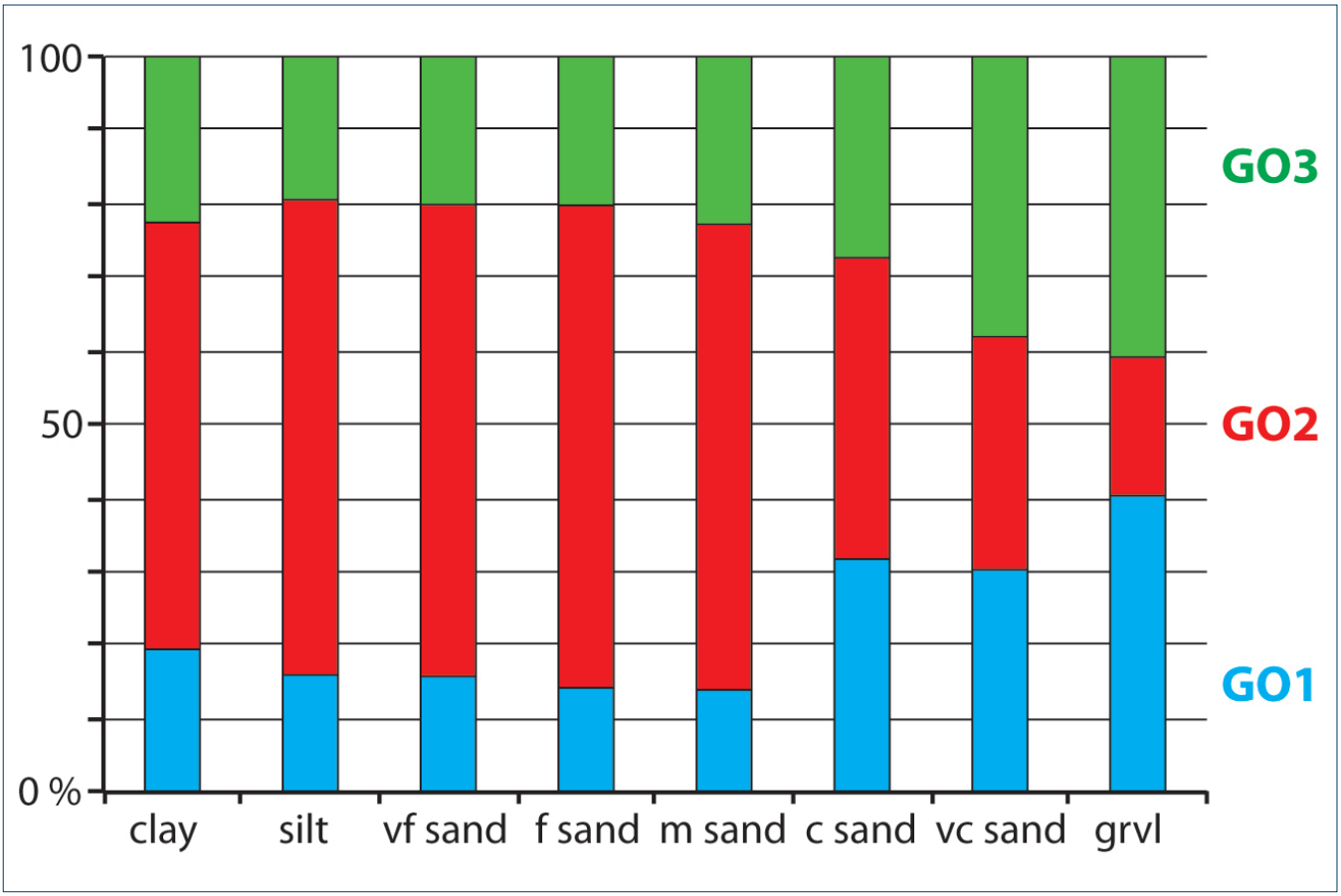

Fig. 4. Grain size distributions normalized to proportions in each respective size bin for samples GO1, GO2, GO3.

B. Sample GO4

Sample GO4 consists of pebble- and cobble-sized clasts (Fig. 6). These were examined visually and identified and grouped by lithic type (igneous, metamorphic or sedimentary). The dominant clasts are derived from chalk-flint lithologies; some of these exhibit a greenish tinge, likely reflecting a glauconitic-chloritic component (although K is not shown as being abundant in the XRF analyses, see below). The next most abundant are calcareous and dolomitic grainstone followed by mafic and intermediate composition volcanites (likely basaltic/andesitic) and meta-igneous rocks (gneissic granitoids and meta-felsites). Two small pieces of rusted iron were noted.

Although determining provenance from such a limited analyses is speculative, if the varied lithologies are derived from the same source region then the association of chalk, flint, calc/doloarenite, mafic volcanites and meta-felsic rocks implies a geological terrane in which there are Cretaceous sedimentary units (the chalk-flint-calc/doloarenite assemblage) and metamorphosed basement rocks and volcanics. A cursory examination of the geology surrounding the North Sea implies that a plausible geological match is the Amorican basement-cover sequences of Brittany-Normandy.

4. Geochemical Analyses: Samples GO1, GO2, GO3

The finer than 1mm material of samples GO1, GO2 and GO3 was analyzed using X-Ray Diffractometry (XRD) and X-Ray Fluorescence (XRF) spectrometry. These techniques identify, respectively, the mineralogical composition and the major and trace element and oxide species present (Tables 2-4, Fig. 7).

A. X-Ray Diffraction

The XRD analyses (Table 2, Fig. 7) show that the mineralogy of samples GO1, GO2 and GO3 is dominated by carbonate minerals (calcite/aragonite and Mg-calcite/dolomite), followed by silicate minerals (quartz and traces of plagioclase feldspar) and then minor to trace amounts of an evaporate mineral (halite).

This reflects the bulk composition of the material as noted visually, namely the abundance of carbonate lithologies (chalk, calcarenite, Mg-calcite/dolomite) and shelly marine invertebrate material (calcite, aragonite). The quartz reflects the flint nodules.

B. X-Ray Fluorescence

The XRF analyses (Table 3), as is the case for the XRD data, reflect an expected suite of major and trace elements and oxides given the mineralogy and visual assessment of the grain size material. The major oxides of CaO and

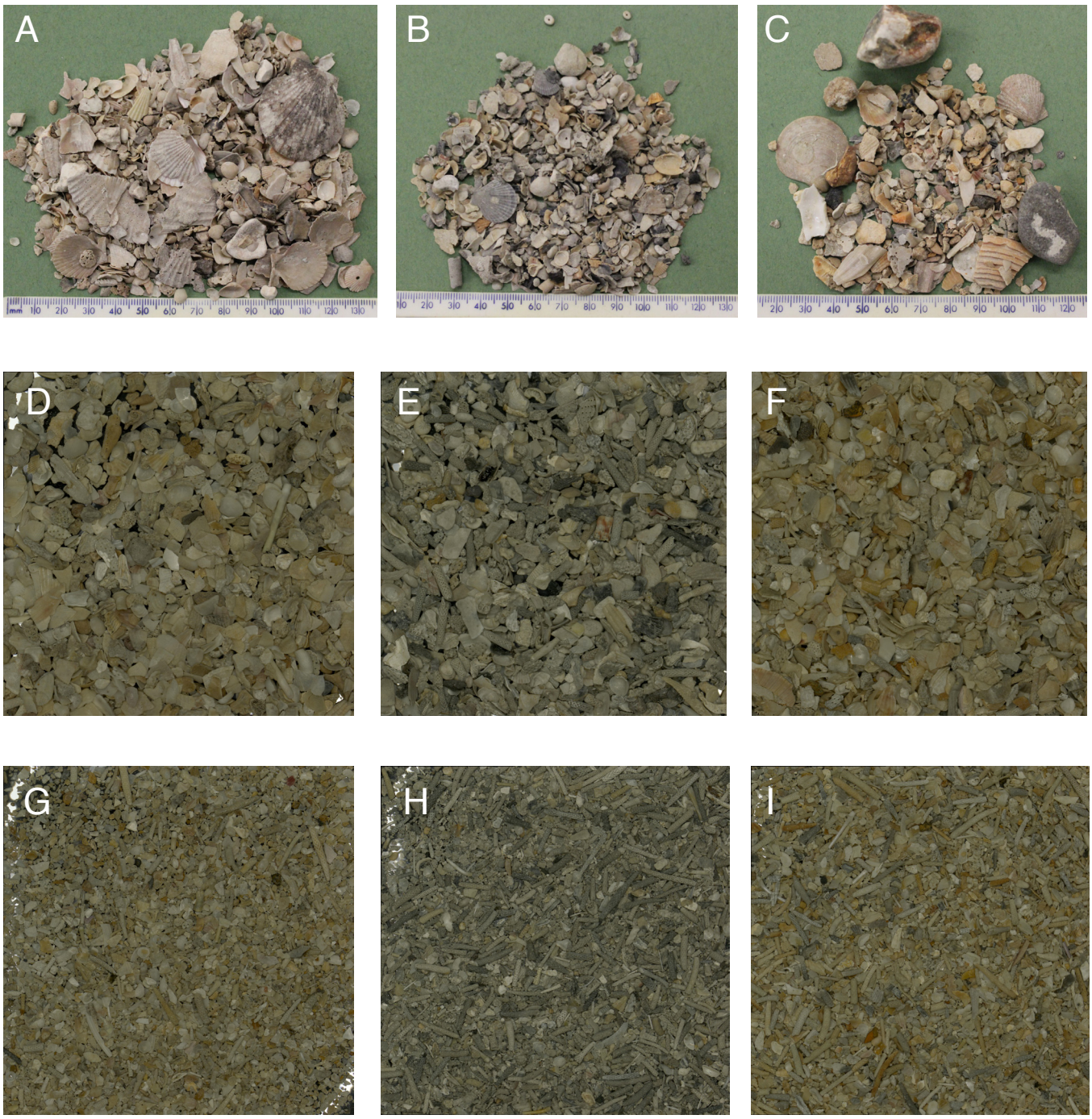

Fig. 5. Images of bioclastic components and fractions greater than 2mm (A, B, C), 1-2mm (D, E, F) and c. 1mm (G, H, I). Sample GO1: A, D, G. Sample GO2: B, E, H. Sample GO3: C, F, I. Note the abundance of shelly material derived from broken fragments of epifaunal and infaunal species.

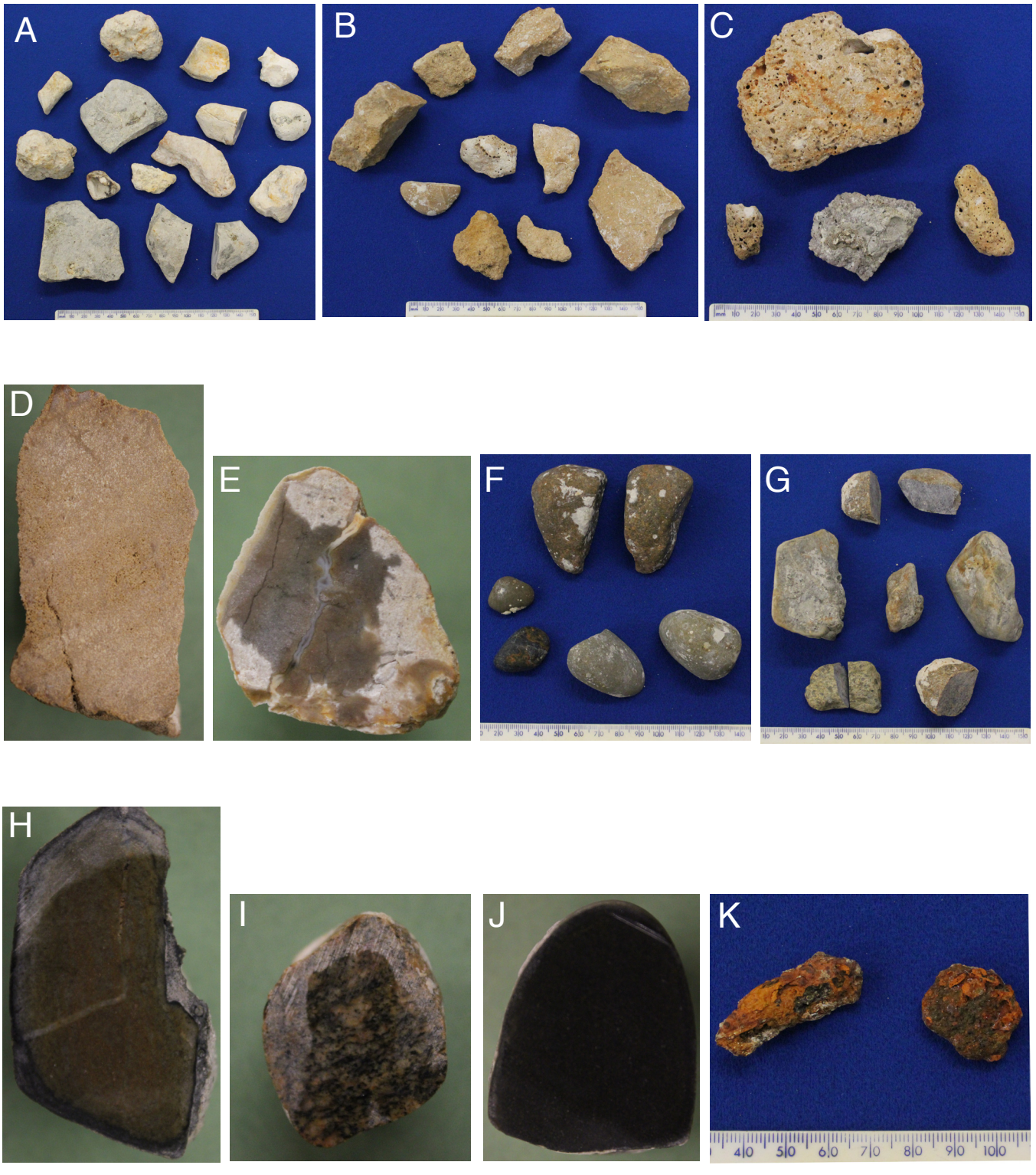

Fig. 6. Cobbles and pebbles of sample GO4. A. Chalk-flint lithologies (note greenish tinge on some clasts). B. Calc/doloarenitc grainstones and packstones. C. Calcarenitic clasts that have undergone intensive boring. D. Close-up of dolomitic calcarenitic clast showing sedimentary layering. E. Close-up of flint clast. F. Mafic and intermediate volcanite clasts; note how well rounded some clasts are. G. Meta-igneous clasts; meta-felsites and gneissic granitoids. H. Close-up of meta-felsite clast. I. Close-up of granitic gneiss clast. J. Close-up of basalt clast. K. Deeply corroded and rusted iron fragments. Note that one or two clasts from each clast assemblage were cut to better display textural features.

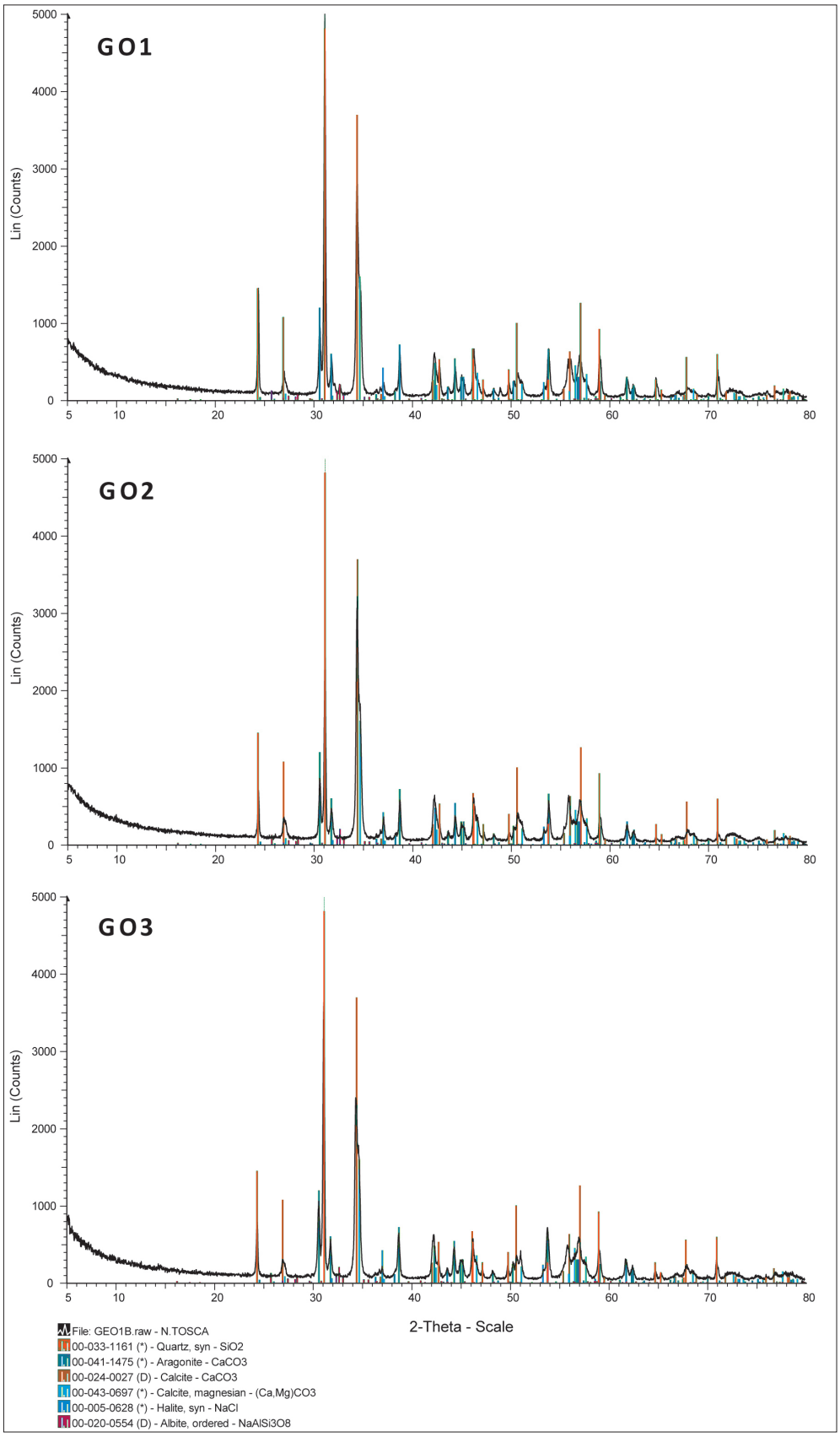

Fig. 7. X-Ray diffractometer traces based on the mineralogical components of samples GO1, GO2 and GO3.

SiO_2 show the dominance of materials derived from the shelly fragments and the chalk-flint lithologies. The minor amounts of MgO and Fe_2O_3 are likely indicating the presence of dolomite and rust particles, the latter most probably derived from the wreck. The even lesser amounts of Na_2O and K_2O record the presence of minor amounts of plagioclase and/or halite and feasibly glauconite. The trace element data are similarly compatible with the XRD and visually assessed data for composition of the samples.

5. Summary & Conclusions

Grain size and XRD/F analyses were performed on four samples (GO1, GO2, GO3, GO4) obtained in 2012 from the seabed associated with the wreck of the *Victory* (site 25C). Beckman-Coulter LS-230 laser granulometry revealed a dearth of material finer than coarse sand and determined that the dominant grain size distributions were *c*. 1 mm and larger (up to pebble and cobble sizes). Visual identification of the largest size fractions showed four main lithological associations, in decreasing order of abundance these are: (i) chalk-flint; (ii) calc/doloarenitic grainstone; (iii) mafic and intermediate volcanites; and (iv) meta-felsic igneous clasts. Fragments of broken and abraded bivalves, bryozoan, barnacles, crustaceans and regular echinoids tests dominated the biological component. Geochemical analyses corroborated the visual inspections, showing that the mineralogy was mostly calcite/aragonite and quartz, with minor dolomite and lesser plagioclase and halite.

Visual and geophysical imagery of site 25C identifies the presence of large bedforms. Combined with the coarse nature of the sediments, which are indicative of the action of strong currents, conditions are hence likely to be well aerated. As such, site 25C would not be an optimum setting for the anaerobic preservation of artifacts.

Many of the shell fragments examined showed evidence of boring, while some of the gravel-sized fragments in sample GO4, taken closest to the natural hardpan substrate, contained burrows. Thus, the inorganic components of the field site show evidence of in/epifaunal activity, leading to the assumption that organic remains such as wood would likely be subject to similar activity. The entire sedimentological sample set of G01 to G04 gives the impression of being extensively sorted and dynamic, which is also evident from side-scan sonar and multibeam imagery of large bedforms indicating a mobile substrate.

Appendix A. Beckman-Coulter LS-230 laser granulometer grain size analyses for samples GO1, GO2 and GO3.

File name:	GO1__dah_132.$ls	File name:	GO1__dah_133.$ls	File name:	GO1__dah_134.$ls
File ID:	GO1	File ID:	GO1	File ID:	GO1
Sample ID:		Sample ID:		Sample ID:	
Operator:	dah	Operator:	dah	Operator:	dah
Bar code:		Bar code:		Bar code:	
Comment 1:		Comment 1:		Comment 1:	
Comment 2:	GO1	Comment 2:	GO1	Comment 2:	GO1
Instrument:	LS 230, Fluid Module	Instrument:	LS 230, Fluid Module	Instrument:	LS 230, Fluid Module
Run number:	132	Run number:	133	Run number:	134
Run length:	60	Run length:	60	Run length:	61
Optical model:	Fraunhofer.rfd	Optical model:	Fraunhofer.rfd	Optical model:	Fraunhofer.rfd
Obscuration:	11	Obscuration:	11	Obscuration:	11
PIDS Obscur:		PIDS Obscur:		PIDS Obscur:	
Obscuration:	OK	Obscuration:	OK	Obscuration:	OK
Serial Number:	6987	Serial Number:	6987	Serial Number:	6987
From	0.375	From	0.375	From	0.375
To	2000	To	2000	To	2000
Volume	100	Volume	100	Volume	100
Mean:	659.7	Mean:	655.5	Mean:	647.4
Median:	551.7	Median:	547.1	Median:	543
D(3,2):	234.4	D(3,2):	225.5	D(3,2):	216
Mean/Median ratio:	1.196	Mean/Median ratio:	1.198	Mean/Median ratio:	1.192
Mode:	471.1	Mode:	471.1	Mode:	471.1
S.D.:	391.3	S.D.:	390.4	S.D.:	382.3
Variance:	1.53E+05	Variance:	1.52E+05	Variance:	1.46E+05
C.V.:	59.32	C.V.:	59.56	C.V.:	59.06
Skewness:	1.043	Skewness:	1.067	Skewness:	1.062
Kurtosis:	0.636	Kurtosis:	0.71	Kurtosis:	0.752
d10:	262.2	d10:	261.8	d10:	260.5
d50:	551.7	d50:	547.1	d50:	543
d90:	1237	d90:	1231	d90:	1209
Specific Surf. Area:	256	Specific Surf. Area:	266	Specific Surf. Area:	277.8
% <	Size	% <	Size	% <	Size
10	262	10	262	10	261
25	369	25	367	25	365
50	552	50	547	50	543
75	874	75	864	75	854
90	1237	90	1231	90	1209
% >	Size	% >	Size	% >	Size
10	1237	10	1231	10	1209
25	874	25	864	25	854
50	552	50	547	50	543
75	369	75	367	75	365

CERSA Centre for Earth Resources St Andrews

Sediment Analysis Report: HMS Victory Site 25c

90	262	90	262	90	261
Size	% <	Size	% <	Size	% <
1	0.018	1	0.019	1	0.021
10	0.48	10	0.51	10	0.56
100	1.29	100	1.35	100	1.44
1000	81.3	1000	81.7	1000	82.4
Size	% >	Size	% >	Size	% >
1	99.98	1	99.98	1	99.98
10	99.5	10	99.5	10	99.4
100	98.7	100	98.6	100	98.6
1000	18.7	1000	18.3	1000	17.6
Particle Diameter	GO1__dah_132.$ls	Particle Diameter	GO1__dah_133.$ls	Particle Diameter	GO1__dah_134.$ls
um	Volume	um	Volume	um	Volume
	% <		% <		% <
0.782	0.00018	0.782	0.0002	0.782	0.00021
1	0.018	1	0.019	1	0.021
2	0.16	2	0.18	2	0.19
3	0.23	3	0.25	3	0.27
4	0.28	4	0.3	4	0.32
5	0.32	5	0.34	5	0.37
7	0.39	7	0.42	7	0.46
10	0.48	10	0.51	10	0.56
20	0.63	20	0.69	20	0.75
40	0.82	40	0.88	40	0.95
80	1.11	80	1.17	80	1.25
82.72	1.13	82.72	1.19	82.72	1.28
Channel Diameter (Lower)	Diff.	Channel Diameter (Lower)	Diff.	Channel Diameter (Lower)	Diff.
um	Volume	um	Volume	um	Volume
	%		%		%
0.375	0	0.375	0	0.375	0
0.412	0	0.412	0	0.412	0
0.452	0	0.452	0	0.452	0
0.496	0	0.496	0	0.496	0
0.545	0	0.545	0	0.545	0
0.598	0	0.598	0	0.598	0
0.656	0	0.656	0	0.656	0
0.721	0.00021	0.721	0.00022	0.721	0.00024
0.791	0.0028	0.791	0.003	0.791	0.0032
0.868	0.0084	0.868	0.009	0.868	0.0097
0.953	0.013	0.953	0.014	0.953	0.016
1.047	0.017	1.047	0.018	1.047	0.02
1.149	0.02	1.149	0.021	1.149	0.023
1.261	0.021	1.261	0.023	1.261	0.025
1.385	0.022	1.385	0.023	1.385	0.025
1.52	0.021	1.52	0.023	1.52	0.024
1.668	0.02	1.668	0.022	1.668	0.023
1.832	0.019	1.832	0.02	1.832	0.022
2.011	0.017	2.011	0.019	2.011	0.02

CERSA Centre for Earth Resources St Andrews

Sediment Analysis Report: : HMS Victory Site 25c

2.207	0.016	2.207	0.017	2.207	0.019
2.423	0.015	2.423	0.016	2.423	0.017
2.66	0.014	2.66	0.015	2.66	0.017
2.92	0.014	2.92	0.015	2.92	0.017
3.205	0.014	3.205	0.016	3.205	0.017
3.519	0.015	3.519	0.016	3.519	0.018
3.863	0.016	3.863	0.017	3.863	0.019
4.24	0.017	4.24	0.018	4.24	0.02
4.655	0.018	4.655	0.02	4.655	0.022
5.11	0.019	5.11	0.021	5.11	0.023
5.61	0.02	5.61	0.022	5.61	0.024
6.158	0.021	6.158	0.023	6.158	0.025
6.76	0.022	6.76	0.024	6.76	0.026
7.421	0.022	7.421	0.024	7.421	0.026
8.147	0.022	8.147	0.024	8.147	0.026
8.943	0.022	8.943	0.024	8.943	0.026
9.817	0.022	9.817	0.024	9.817	0.026
10.78	0.022	10.78	0.023	10.78	0.025
11.83	0.021	11.83	0.023	11.83	0.025
12.99	0.021	12.99	0.023	12.99	0.025
14.26	0.021	14.26	0.023	14.26	0.025
15.65	0.021	15.65	0.023	15.65	0.025
17.18	0.022	17.18	0.023	17.18	0.025
18.86	0.022	18.86	0.023	18.86	0.025
20.7	0.022	20.7	0.023	20.7	0.025
22.73	0.022	22.73	0.023	22.73	0.025
24.95	0.023	24.95	0.024	24.95	0.025
27.39	0.024	27.39	0.025	27.39	0.026
30.07	0.026	30.07	0.026	30.07	0.028
33.01	0.028	33.01	0.029	33.01	0.03
36.24	0.03	36.24	0.03	36.24	0.032
39.78	0.031	39.78	0.031	39.78	0.033
43.67	0.031	43.67	0.032	43.67	0.033
47.94	0.033	47.94	0.033	47.94	0.034
52.62	0.036	52.62	0.036	52.62	0.037
57.77	0.04	57.77	0.041	57.77	0.042
63.41	0.045	63.41	0.046	63.41	0.048
69.61	0.05	69.61	0.051	69.61	0.052
76.42	0.057	76.42	0.057	76.42	0.058
83.89	0.07	83.89	0.069	83.89	0.071
92.09	0.09	92.09	0.089	92.09	0.091
101.1	0.12	101.1	0.12	101.1	0.12
111	0.15	111	0.15	111	0.15
121.8	0.2	121.8	0.2	121.8	0.2
133.7	0.28	133.7	0.28	133.7	0.27
146.8	0.4	146.8	0.4	146.8	0.4
161.2	0.6	161.2	0.59	161.2	0.59
176.9	0.88	176.9	0.87	176.9	0.88
194.2	1.28	194.2	1.27	194.2	1.28
213.2	1.78	213.2	1.78	213.2	1.8
234.1	2.38	234.1	2.39	234.1	2.42
256.9	3.05	256.9	3.09	256.9	3.11
282.1	3.76	282.1	3.82	282.1	3.85

CERSA Centre for Earth Resources St Andrews

Sediment Analysis Report: HMS Victory Site 25c

309.6	4.45	309.6	4.53	309.6	4.56
339.9	5.07	339.9	5.15	339.9	5.18
373.1	5.56	373.1	5.63	373.1	5.67
409.6	5.86	409.6	5.92	409.6	5.96
449.7	5.96	449.7	6	449.7	6.05
493.6	5.87	493.6	5.9	493.6	5.95
541.9	5.64	541.9	5.66	541.9	5.71
594.9	5.34	594.9	5.36	594.9	5.41
653	5.05	653	5.07	653	5.11
716.8	4.82	716.8	4.82	716.8	4.87
786.9	4.65	786.9	4.61	786.9	4.65
863.9	4.47	863.9	4.4	863.9	4.44
948.3	4.26	948.3	4.16	948.3	4.18
1041	3.92	1041	3.81	1041	3.8
1143	3.45	1143	3.35	1143	3.31
1255	2.9	1255	2.82	1255	2.75
1377	2.31	1377	2.26	1377	2.14
1512	1.79	1512	1.76	1512	1.62
1660	1.38	1660	1.38	1660	1.22
1822	1.06	1822	1.08	1822	0.91

File name:	GO2__dah_135.$ls	File name:	GO2__dah_136.$ls	File name:	GO2__dah_137.$ls
File ID:	GO2	File ID:	GO2	File ID:	GO2
Sample ID:		Sample ID:		Sample ID:	
Operator:	dah	Operator:	dah	Operator:	dah
Bar code:		Bar code:		Bar code:	
Comment 1:		Comment 1:		Comment 1:	
Comment 2:	GO2	Comment 2:	GO2	Comment 2:	GO2
Instrument:	LS 230, Fluid Module	Instrument:	LS 230, Fluid Module	Instrument:	LS 230, Fluid Module
Run number:	135	Run number:	136	Run number:	137
Run length:	60	Run length:	60	Run length:	60
Optical model:	Fraunhofer.rfd	Optical model:	Fraunhofer.rfd	Optical model:	Fraunhofer.rfd
Obscuration:	13	Obscuration:	13	Obscuration:	14
PIDS Obscur:		PIDS Obscur:		PIDS Obscur:	
Obscuration:	High	Obscuration:	High	Obscuration:	High
Serial Number:	6987	Serial Number:	6987	Serial Number:	6987
From	0.375	From	0.375	From	0.375
To	2000	To	2000	To	2000
Volume	100	Volume	100	Volume	100
Mean:	553.1	Mean:	554	Mean:	552.1
Median:	458.4	Median:	453.2	Median:	457.5
D(3,2):	125.8	D(3,2):	104.9	D(3,2):	103.7
Mean/Median ratio:	1.207	Mean/Median ratio:	1.222	Mean/Median ratio:	1.207
Mode:	429.2	Mode:	429.2	Mode:	429.2
S.D.:	355	S.D.:	367.1	S.D.:	356.6
Variance:	1.26E+05	Variance:	1.35E+05	Variance:	1.27E+05
C.V.:	64.19	C.V.:	66.27	C.V.:	64.6
Skewness:	1.163	Skewness:	1.223	Skewness:	1.146
Kurtosis:	1.197	Kurtosis:	1.345	Kurtosis:	1.175
d10:	205.2	d10:	200.6	d10:	202

CERSA Centre for Earth Resources St Andrews

Sediment Analysis Report: : HMS Victory Site 25c

CERSA Centre for Earth Resources St Andrews

Sediment Analysis Report: HMS Victory Site 25c

d50:	458.4	d50:	453.2	d50:	457.5
d90:	1078	d90:	1097	d90:	1077
Specific Surf. Area:	476.9	Specific Surf. Area:	572.2	Specific Surf. Area:	578.8

% <	Size	% <	Size	% <	Size
10	205	10	201	10	202
25	305	25	301	25	304
50	458	50	453	50	457
75	721	75	718	75	724
90	1078	90	1097	90	1077

% >	Size	% >	Size	% >	Size
10	1078	10	1097	10	1077
25	721	25	718	25	724
50	458	50	453	50	457
75	305	75	301	75	304
90	205	90	201	90	202

Size	% <	Size	% <	Size	% <
1	0.039	1	0.14	1	0.15
10	1.3	10	1.51	10	1.54
100	3.95	100	4.38	100	4.38
1000	87.5	1000	87.1	1000	87.5

Size	% >	Size	% >	Size	% >
1	99.96	1	99.9	1	99.9
10	98.7	10	98.5	10	98.5
100	96.1	100	95.6	100	95.6
1000	12.5	1000	12.9	1000	12.5

Particle Diameter um	GO2__dah_135.$ls Volume % <	Particle Diameter um	GO2__dah_136.$ls Volume % <	Particle Diameter um	GO2__dah_137.$ls Volume % <
0.782	0.00039	0.782	0.058	0.782	0.059
1	0.039	1	0.14	1	0.15
2	0.35	2	0.42	2	0.43
3	0.52	3	0.61	3	0.62
4	0.65	4	0.77	4	0.79
5	0.79	5	0.93	5	0.95
7	1.03	7	1.2	7	1.22
10	1.3	10	1.51	10	1.54
20	1.89	20	2.17	20	2.2
40	2.56	40	2.9	40	2.94
80	3.49	80	3.9	80	3.91
82.72	3.55	82.72	3.96	82.72	3.97

Channel Diameter (Lower) um	Diff. Volume %	Channel Diameter (Lower) um	Diff. Volume %	Channel Diameter (Lower) um	Diff. Volume %
0.375	0	0.375	0	0.375	0
0.412	0	0.412	0	0.412	0
0.452	0	0.452	0	0.452	0

CERSA Centre for Earth Resources St Andrews

Sediment Analysis Report: : HMS Victory Site 25c

0.496	0	0.496	0.00029	0.496	0.0003
0.545	0	0.545	0.0039	0.545	0.004
0.598	0	0.598	0.012	0.598	0.012
0.656	0	0.656	0.019	0.656	0.02
0.721	0.00045	0.721	0.026	0.721	0.026
0.791	0.006	0.791	0.031	0.791	0.031
0.868	0.018	0.868	0.035	0.868	0.035
0.953	0.029	0.953	0.037	0.953	0.038
1.047	0.037	1.047	0.038	1.047	0.039
1.149	0.042	1.149	0.038	1.149	0.039
1.261	0.045	1.261	0.038	1.261	0.039
1.385	0.046	1.385	0.038	1.385	0.038
1.52	0.045	1.52	0.037	1.52	0.038
1.668	0.043	1.668	0.037	1.668	0.038
1.832	0.041	1.832	0.037	1.832	0.038
2.011	0.039	2.011	0.038	2.011	0.039
2.207	0.038	2.207	0.04	2.207	0.041
2.423	0.038	2.423	0.043	2.423	0.043
2.66	0.039	2.66	0.046	2.66	0.046
2.92	0.041	2.92	0.049	2.92	0.05
3.205	0.043	3.205	0.053	3.205	0.054
3.519	0.047	3.519	0.057	3.519	0.058
3.863	0.051	3.863	0.061	3.863	0.062
4.24	0.055	4.24	0.065	4.24	0.066
4.655	0.059	4.655	0.069	4.655	0.07
5.11	0.063	5.11	0.072	5.11	0.074
5.61	0.066	5.61	0.075	5.61	0.076
6.158	0.069	6.158	0.077	6.158	0.079
6.76	0.071	6.76	0.079	6.76	0.081
7.421	0.072	7.421	0.081	7.421	0.082
8.147	0.073	8.147	0.082	8.147	0.083
8.943	0.074	8.943	0.083	8.943	0.084
9.817	0.074	9.817	0.083	9.817	0.085
10.78	0.075	10.78	0.084	10.78	0.085
11.83	0.076	11.83	0.085	11.83	0.087
12.99	0.077	12.99	0.087	12.99	0.088
14.26	0.079	14.26	0.089	14.26	0.09
15.65	0.081	15.65	0.092	15.65	0.093
17.18	0.083	17.18	0.093	17.18	0.094
18.86	0.084	18.86	0.094	18.86	0.094
20.7	0.083	20.7	0.093	20.7	0.093
22.73	0.083	22.73	0.092	22.73	0.092
24.95	0.084	24.95	0.092	24.95	0.092
27.39	0.086	27.39	0.095	27.39	0.095
30.07	0.091	30.07	0.1	30.07	0.1
33.01	0.098	33.01	0.11	33.01	0.11
36.24	0.1	36.24	0.11	36.24	0.11
39.78	0.11	39.78	0.12	39.78	0.12
43.67	0.11	43.67	0.12	43.67	0.12
47.94	0.11	47.94	0.12	47.94	0.12
52.62	0.12	52.62	0.12	52.62	0.12
57.77	0.13	57.77	0.14	57.77	0.13
63.41	0.14	63.41	0.15	63.41	0.14

CERSA Centre for Earth Resources St Andrews

Sediment Analysis Report: HMS Victory Site 25c

69.61	0.15	69.61	0.16	69.61	0.15
76.42	0.16	76.42	0.17	76.42	0.16
83.89	0.18	83.89	0.19	83.89	0.19
92.09	0.22	92.09	0.23	92.09	0.22
101.1	0.26	101.1	0.27	101.1	0.26
111	0.31	111	0.32	111	0.31
121.8	0.39	121.8	0.4	121.8	0.39
133.7	0.53	133.7	0.54	133.7	0.53
146.8	0.75	146.8	0.76	146.8	0.74
161.2	1.07	161.2	1.08	161.2	1.05
176.9	1.51	176.9	1.52	176.9	1.48
194.2	2.07	194.2	2.08	194.2	2.03
213.2	2.71	213.2	2.73	213.2	2.68
234.1	3.39	234.1	3.43	234.1	3.37
256.9	4.07	256.9	4.12	256.9	4.06
282.1	4.71	282.1	4.75	282.1	4.7
309.6	5.26	309.6	5.3	309.6	5.25
339.9	5.7	339.9	5.72	339.9	5.68
373.1	5.99	373.1	5.99	373.1	5.95
409.6	6.1	409.6	6.09	409.6	6.05
449.7	6.01	449.7	5.97	449.7	5.95
493.6	5.71	493.6	5.64	493.6	5.64
541.9	5.25	541.9	5.14	541.9	5.17
594.9	4.72	594.9	4.59	594.9	4.66
653	4.26	653	4.1	653	4.22
716.8	3.89	716.8	3.72	716.8	3.9
786.9	3.63	786.9	3.44	786.9	3.68
863.9	3.43	863.9	3.24	863.9	3.49
948.3	3.23	948.3	3.08	948.3	3.3
1041	2.95	1041	2.85	1041	2.98
1143	2.54	1143	2.51	1143	2.54
1255	2.07	1255	2.11	1255	2.05
1377	1.53	1377	1.62	1377	1.5
1512	1.01	1512	1.14	1512	0.98
1660	0.6	1660	0.78	1660	0.6
1822	0.36	1822	0.55	1822	0.38

File name:	GO3__dah_138.$ls	File name:	GO3__dah_139.$ls	File name:	GO3__dah_140.$ls
File ID:	GO3	File ID:	GO3	File ID:	GO3
Sample ID:		Sample ID:		Sample ID:	
Operator:	dah	Operator:	dah	Operator:	dah
Bar code:		Bar code:		Bar code:	
Comment 1:		Comment 1:		Comment 1:	
Comment 2:	GO3	Comment 2:	GO3	Comment 2:	GO3
Instrument:	LS 230, Fluid Module	Instrument:	LS 230, Fluid Module	Instrument:	LS 230, Fluid Module
Run number:	138	Run number:	139	Run number:	140
Run length:	61	Run length:	60	Run length:	61
Optical model:	Fraunhofer.rfd	Optical model:	Fraunhofer.rfd	Optical model:	Fraunhofer.rfd
Obscuration:	11	Obscuration:	11	Obscuration:	11
PIDS Obscur:		PIDS Obscur:		PIDS Obscur:	
Obscuration:	OK	Obscuration:	OK	Obscuration:	OK
Serial Number:	6987	Serial Number:	6987	Serial Number:	6987

CERSA Centre for Earth Resources St Andrews

Sediment Analysis Report: : HMS Victory Site 25c

CERSA Centre for Earth Resources St Andrews

Sediment Analysis Report: HMS Victory Site 25c

From	0.375	From	0.375	From	0.375
To	2000	To	2000	To	2000
Volume	100	Volume	100	Volume	100
Mean:	664.5	Mean:	666.6	Mean:	656.7
Median:	562.4	Median:	564.2	Median:	557.7
D(3,2):	195	D(3,2):	188.1	D(3,2):	179.8
Mean/Median ratio:	1.182	Mean/Median ratio:	1.181	Mean/Median ratio:	1.178
Mode:	471.1	Mode:	471.1	Mode:	471.1
S.D.:	396.8	S.D.:	398.6	S.D.:	390.6
Variance:	1.58E+05	Variance:	1.59E+05	Variance:	1.53E+05
C.V.:	59.72	C.V.:	59.79	C.V.:	59.47
Skewness:	0.915	Skewness:	0.91	Skewness:	0.907
Kurtosis:	0.344	Kurtosis:	0.339	Kurtosis:	0.364
d10:	251.4	d10:	251.6	d10:	249.5
d50:	562.4	d50:	564.2	d50:	557.7
d90:	1246	d90:	1247	d90:	1228
Specific Surf. Area:	307.8	Specific Surf. Area:	319	Specific Surf. Area:	333.7

% <	Size	% <	Size	% <	Size
10	251	10	252	10	250
25	365	25	365	25	362
50	562	50	564	50	558
75	902	75	906	75	891
90	1246	90	1247	90	1228

% >	Size	% >	Size	% >	Size
10	1246	10	1247	10	1228
25	902	25	906	25	891
50	562	50	564	50	558
75	365	75	365	75	362
90	251	90	252	90	250

Size	% <	Size	% <	Size	% <
1	0.025	1	0.027	1	0.029
10	0.66	10	0.7	10	0.76
100	2.13	100	2.22	100	2.32
1000	80.2	1000	80	1000	80.8

Size	% >	Size	% >	Size	% >
1	99.98	1	99.97	1	99.97
10	99.3	10	99.3	10	99.2
100	97.9	100	97.8	100	97.7
1000	19.8	1000	20	1000	19.2

Particle Diameter um	GO3__dah_138.$ls Volume % <	Particle Diameter um	GO3__dah_139.$ls Volume % <	Particle Diameter um	GO3__dah_140.$ls Volume % <
0.782	0.00025	0.782	0.00027	0.782	0.00029
1	0.025	1	0.027	1	0.029
2	0.22	2	0.23	2	0.25
3	0.31	3	0.33	3	0.35
4	0.37	4	0.4	4	0.42

CERSA Centre for Earth Resources St Andrews

Sediment Analysis Report: : HMS Victory Site 25c

CERSA Centre for Earth Resources St Andrews

Sediment Analysis Report: HMS Victory Site 25c

5	0.43	5	0.46	5	0.49
7	0.53	7	0.57	7	0.61
10	0.66	10	0.7	10	0.76
20	0.91	20	0.97	20	1.05
40	1.24	40	1.32	40	1.41
80	1.82	80	1.9	80	2.01
82.72	1.86	82.72	1.94	82.72	2.05

Channel Diameter (Lower) um	Diff. Volume %	Channel Diameter (Lower) um	Diff. Volume %	Channel Diameter (Lower) um	Diff. Volume %
0.375	0	0.375	0	0.375	0
0.412	0	0.412	0	0.412	0
0.452	0	0.452	0	0.452	0
0.496	0	0.496	0	0.496	0
0.545	0	0.545	0	0.545	0
0.598	0	0.598	0	0.598	0
0.656	0	0.656	0	0.656	0
0.721	0.00029	0.721	0.00031	0.721	0.00033
0.791	0.0038	0.791	0.0041	0.791	0.0044
0.868	0.012	0.868	0.012	0.868	0.013
0.953	0.018	0.953	0.02	0.953	0.021
1.047	0.024	1.047	0.025	1.047	0.027
1.149	0.027	1.149	0.029	1.149	0.031
1.261	0.029	1.261	0.031	1.261	0.033
1.385	0.029	1.385	0.031	1.385	0.033
1.52	0.028	1.52	0.03	1.52	0.032
1.668	0.027	1.668	0.028	1.668	0.03
1.832	0.025	1.832	0.026	1.832	0.028
2.011	0.023	2.011	0.024	2.011	0.026
2.207	0.021	2.207	0.022	2.207	0.024
2.423	0.02	2.423	0.021	2.423	0.022
2.66	0.019	2.66	0.02	2.66	0.022
2.92	0.019	2.92	0.02	2.92	0.022
3.205	0.019	3.205	0.021	3.205	0.023
3.519	0.021	3.519	0.022	3.519	0.024
3.863	0.022	3.863	0.024	3.863	0.026
4.24	0.024	4.24	0.026	4.24	0.028
4.655	0.026	4.655	0.028	4.655	0.03
5.11	0.027	5.11	0.03	5.11	0.032
5.61	0.029	5.61	0.031	5.61	0.034
6.158	0.03	6.158	0.033	6.158	0.035
6.76	0.031	6.76	0.034	6.76	0.036
7.421	0.032	7.421	0.034	7.421	0.037
8.147	0.032	8.147	0.035	8.147	0.037
8.943	0.033	8.943	0.035	8.943	0.038
9.817	0.033	9.817	0.035	9.817	0.038
10.78	0.033	10.78	0.035	10.78	0.038
11.83	0.033	11.83	0.035	11.83	0.038
12.99	0.034	12.99	0.036	12.99	0.038
14.26	0.035	14.26	0.037	14.26	0.039
15.65	0.036	15.65	0.038	15.65	0.04
17.18	0.036	17.18	0.039	17.18	0.041

CERSA Centre for Earth Resources St Andrews

Sediment Analysis Report: : HMS Victory Site 25c

18.86	0.037	18.86	0.039	18.86	0.042
20.7	0.038	20.7	0.04	20.7	0.042
22.73	0.038	22.73	0.04	22.73	0.043
24.95	0.04	24.95	0.042	24.95	0.044
27.39	0.042	27.39	0.044	27.39	0.046
30.07	0.046	30.07	0.048	30.07	0.051
33.01	0.051	33.01	0.053	33.01	0.056
36.24	0.056	36.24	0.058	36.24	0.06
39.78	0.061	39.78	0.062	39.78	0.064
43.67	0.064	43.67	0.065	43.67	0.066
47.94	0.067	47.94	0.068	47.94	0.069
52.62	0.072	52.62	0.073	52.62	0.074
57.77	0.079	57.77	0.081	57.77	0.083
63.41	0.088	63.41	0.09	63.41	0.093
69.61	0.097	69.61	0.099	69.61	0.1
76.42	0.11	76.42	0.11	76.42	0.11
83.89	0.13	83.89	0.13	83.89	0.13
92.09	0.15	92.09	0.15	92.09	0.15
101.1	0.18	101.1	0.17	101.1	0.18
111	0.21	111	0.2	111	0.21
121.8	0.26	121.8	0.25	121.8	0.25
133.7	0.33	133.7	0.32	133.7	0.33
146.8	0.45	146.8	0.44	146.8	0.45
161.2	0.64	161.2	0.63	161.2	0.64
176.9	0.92	176.9	0.91	176.9	0.92
194.2	1.3	194.2	1.28	194.2	1.3
213.2	1.78	213.2	1.77	213.2	1.79
234.1	2.36	234.1	2.34	234.1	2.37
256.9	2.99	256.9	2.96	256.9	3.01
282.1	3.63	282.1	3.62	282.1	3.66
309.6	4.25	309.6	4.24	309.6	4.29
339.9	4.79	339.9	4.79	339.9	4.83
373.1	5.2	373.1	5.21	373.1	5.25
409.6	5.47	409.6	5.46	409.6	5.51
449.7	5.56	449.7	5.53	449.7	5.59
493.6	5.49	493.6	5.43	493.6	5.51
541.9	5.32	541.9	5.23	541.9	5.32
594.9	5.1	594.9	5.02	594.9	5.1
653	4.93	653	4.88	653	4.95
716.8	4.82	716.8	4.84	716.8	4.87
786.9	4.77	786.9	4.84	786.9	4.84
863.9	4.72	863.9	4.82	863.9	4.78
948.3	4.59	948.3	4.68	948.3	4.62
1041	4.3	1041	4.34	1041	4.27
1143	3.8	1143	3.8	1143	3.73
1255	3.18	1255	3.16	1255	3.09
1377	2.46	1377	2.45	1377	2.36
1512	1.82	1512	1.83	1512	1.7
1660	1.31	1660	1.34	1660	1.17
1822	0.93	1822	0.98	1822	0.79